Journal Name

ARTICLE

Electrochemistry of $Fe^{3+/2+}$ at Highly Oriented Pyrolytic Graphite (HOPG) Electrodes: Kinetics, Identification of Major Electroactive Sites and Time Effects on the Response†

Received 00th January 20xx,
Accepted 00th January 20xx

DOI: 10.1039/x0xx00000x

www.rsc.org/

Guohui Zhang,[a] Sze-yin Tan,[a,b] Anisha N. Patel,[a,c] and Patrick R. Unwin[a,*]

The electrochemistry of the $Fe^{3+/2+}$ redox couple has been studied on highly oriented pyrolytic graphite (HOPG) samples that differ in step edge density by 2 orders of magnitude to elucidate the effect of surface structure on the electron transfer (ET) kinetics. Macroscopic cyclic voltammetry measurements in a droplet-cell arrangement, highlight that the $Fe^{3+/2+}$ process is characterised by slow ET kinetics on HOPG and that step edge coverage has little effect on the electrochemistry of $Fe^{3+/2+}$. A standard heterogeneous ET rate constant of ~5×10^{-5} cm s^{-1} for freshly cleaved HOPG was derived from simulation of the experimental results, which fell into the range of the values reported for metal eletrodes, e.g. platinum and gold, despite the remarkable difference in density of electronic states (DOS) between HOPG and metal electrodes. This provides further evidence that outer-sphere redox processes on metal and sp^2 carbon electrodes appear to be adiabatic. Complementary surface electroactivity mapping of HOPG, using scanning electrochemical cell microscopy, reveal the basal plane to be the predominant site for the $Fe^{3+/2+}$ redox process. It is found that time after cleavage of the HOPG surface has an impact on the surface wettability (and surface contamination), as determined by contact angle measurements, and that this leads to a slow deterioration of the kinetics. These studies further confirm the importance of understanding and evaluating surface structure and history effects in HOPG electrochemistry, and how high resolution measurements, coupled with macroscopic studies provide a holistic view of electrochemical processes.

Introduction

Carbon electrodes are studied extensively for both fundamental electrochemistry and myriad practical applications.[1-4] Within the family of carbon materials, highly oriented pyrolytic graphite (HOPG) - where sp^2 hybridized carbon atoms in a honeycomb (graphene) arrangement within layers are stacked to make a 3D material - has generated huge research interest. In part, this is because fresh surfaces can be easily prepared, by mechanical or Scotch-tape based exfoliation, to produce well-defined structures, i.e. basal plane (terraces) and step edges that are easily characterised by a variety of techniques.[5, 6] Further, HOPG is generally regarded as a model to which other sp^2 carbon materials, such as carbon nanotubes[7] and graphene,[8, 9] are often compared.

In contrast to early work, which considered the HOPG basal plane to be largely or completely inert, even for outer-sphere redox reactions,[10-14] recent studies have shown that the basal surface of HOPG actually has substantial activity.[2, 3, 5, 15-18] This new finding has come about from a wide range of measurements[2, 3] – macroscopic/microscopic measurements of adsorbed redox species,[17, 19] nanoscopic surface electroactivity imaging,[5, 20-23] and metal nanoparticle nucleation,[24] and for a wide range of redox reactions, including dopamine oxidation,[16, 19] adsorbed anthraquinone reduction,[17] (ferrocenylmethyl)trimethylammonium ($FcTMA^+$) oxidation,[8, 25, 26] $Ru(NH_3)_6^{3+}$ reduction,[5, 8, 18, 20, 22] $IrCl_6^{2-}$ reduction[18] and $Fe(CN)_6^{4-}$ oxidation.[5, 18] In fact, ET kinetics at freshly cleaved HOPG has been shown to be at least as fast as on platinum for $IrCl_6^{2-/3-}$ and $Fe(CN)_6^{4-/3-}$, and the standard heterogeneous ET rate constant (k_0) for $Ru(NH_3)_6^{3+/2+}$ is comparable to that for platinum.[18] Further, the step edge density (which can affect the local density of electronic states[2, 3, 27, 28]) has been found to have little or no impact on the overall ET kinetics of macroscopic HOPG.[15, 19] This various evidence suggests that these processes are adiabatic.[17, 18, 29]

In many of the above-mentioned studies, the reactions of the redox species were so fast (close to reversible) as to be effectively limited by diffusion, and so it was only possible to provide lower limits for k_0.[2, 3, 18] Here, we present a study of the $Fe^{3+/2+}$ redox couple in aqueous solution, which is known to have much slower ET kinetics,[30] but is still regarded as an outer-sphere process,[29] although one that can be promoted (enhanced) by some adsorbed

[a] *Department of Chemistry, University of Warwick, Coventry CV4 7AL, United Kingdom*
[b] *Present address: School of Chemistry, Monash University, Clayton, Victoria 3800, Australia*
[c] *Present address: Interfaces, Traitements, Organisation et Dynamique des Systèmes Laboratory, Sorbonne Paris Cité, Paris Diderot University, CNRS-UMR 7086, 15 rue J. A. Baif, 75013 Paris, France*
* Email: p.r.unwin@warwick.ac.uk
† Electronic Supplementary Information (ESI) available: [details of any supplementary information available should be included here]. See DOI: 10.1039/x0xx00000x

anions at metals such as platinum.[31, 32] Thus, with careful experimental design, this is a very attractive redox system with which to make kinetic comparisons on different electrodes.

In this study, droplet-cell measurements[18, 26] were used to acquire macroscopic cyclic voltammograms (CVs) of $Fe^{3+/2+}$ on two grades (quality) of HOPG that had different step edge coverage (by >2 orders of magnitude). Simulations were performed to interpret the CVs, so as to deduce kinetic values and determine whether step edges had any influence on the kinetics. Scanning electrochemical cell microscopy (SECCM),[33, 34] was then employed to map the electroactivity of high quality (low step density) HOPG, allowing electroactivity maps to be produced that revealed the activity of different local structures, in particular, of the basal surface, free from step edges.

A consideration in HOPG electrochemistry is electrode history effects,[2, 3, 5, 8, 22, 25, 26] particularly the elapsed time after cleavage during which atmospheric contamination can occur.[2, 3, 5, 35] We have addressed this in some detail in our past work,[2, 3, 5, 8, 25, 26] and found that it can quickly play a role for some redox reactions (e.g. $Fe(CN)_6^{4-/3-}$),[5, 20] but the effect on others may be less noticeable. Thus, the possible effect of time after surface cleavage of HOPG, on the electrochemical behaviour of $Fe^{3+/2+}$ has also been briefly explored. The kinetics of the $Fe^{3+/2+}$ couple is sensitive to changes in the surface, when HOPG is left exposed to the air for hours after cleavage and before electrochemical measurements, with the kinetics deteriorating towards values previously reported in the literature for *clean* HOPG (k_0 ~ 1.4 × 10^{-5} cm s^{-1})[11, 36]. However, over short times, for example on the timescale of electrochemical imaging, such effects are negligible.

Experimental

Chemical and Materials

Iron (III) perchlorate hydrate ($Fe(ClO_4)_3 \cdot xH_2O$, 98%) and iron (II) perchlorate hydrate ($Fe(ClO_4)_2 \cdot xH_2O$, 98%) were purchased from Sigma-Aldrich, and perchloric acid ($HClO_4$, 70 % v/v) was obtained from Acros Organics, and used as received. All the solutions were freshly prepared using water purified with a Millipore Milli-Q system (resistivity 18.2 MΩ cm at 25 °C). A high quality, but ungraded HOPG sample was kindly provided by Prof. Richard L. McCreery (University of Alberta, Canada), originating from Dr. Arthur Moore, Union Carbide (now GE Advanced Ceramics) and termed AM grade HOPG herein. SPI-3 grade HOPG was from SPI Supplies (Aztech Trading, UK). The two grades of HOPG used show significant different step edge coverage, by > 2 orders of magnitude, as extensively characterised by atomic force microscopy (AFM) (*vide infra*).[5, 15]

Macroscopic Electrochemistry

A three-electrode setup with a droplet-cell configuration was used for the macroscopic measurements (Figure 1a), in which the HOPG sample was employed as the working electrode (WE), and a platinum wire and a palladium wire (saturated with H_2 at -3 V for 30 min in 0.1 M $HClO_4$), served as the counter electrode (CE) and reference electrode (RE), respectively. Prior to each measurement, HOPG samples were cleaved with Scotch tape to generate a fresh surface, unless otherwise noted. This procedure has been widely used,[5, 19] and shows little difference to other methods of cleavage in terms of surface quality.[19] After cleavage of the HOPG samples, a 20 µL droplet of the solution of interest was gently placed on top of the surface in a quick motion (<3 s), followed by the assembly of the CE and RE into the droplet cell, as was adopted previously.[18, 26] CV measurements were then immediately carried out using a 760C potentiostat (CH Instruments, Inc.), at a range of scan rates of 0.1, 0.5, 1, 2, 3, 4, 5, 6, 7, 8, 9 and 10 V s^{-1} (randomly chosen). For comparison, CVs were also measured using an O-ring (radius 3.1 mm) to confine the contact area of droplet (with a volume of 50 µL) on the WE. Finally, for time effect studies, HOPG was freshly cleaved with Scotch tape and then left exposed to air for different times, i.e. 10 min, 20 min, 30min, 1 h, 2h, 4h, and 12 h, before a droplet was deposited on the surface for CV measurements.

Kinetic Analysis and Simulation

Finite element method (FEM) simulation of the CVs in the droplet-cell configuration were performed in COMSOL Multiphysics 5.1 (COMSOL AB, Sweden), from which the ET kinetics values can be deduced (see more details in ESI,† section S2).

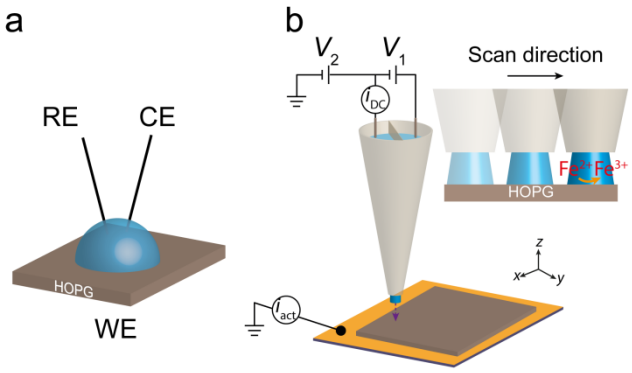

Figure 1. Schematic illustrations of (a) droplet-cell setup for macroscopic cyclic voltammetry and (b) SECCM configuration for surface electroactivity mapping of HOPG.

SECCM Electroactivity Imaging of HOPG

Surface electroactivity mapping of AM HOPG was carried out using an SECCM setup (Figure 1b).[33, 34] A dual-barrel borosilicate theta capillary (1.5 mm o.d., 1.2 mm i.d., TGC150-10, Harvard Apparatus), was pulled with a CO_2 laser puller (P-2000, Sutter Instruments), to produce a tapered dual channel pipet with a total opening of ca. 350 nm across. The pipet was silanized with dimethyldichlorosilane to ensure a hydrophobic outer wall, before being filled with a 2 mM $Fe(ClO_4)_2$ solution, with 0.1 M $HClO_4$ supporting electrolyte. A

palladium wire, saturated with H_2 (produced as above) was then inserted into each barrel, to act as a quasi-reference counter electrode (QRCE). The pipet was mounted on a *z*-piezoelectric positioner and a potential bias (V_1) of 0.2 V was applied between the two QRCEs, generating an ion conductance current (i_{DC}) in the meniscus across the two barrels at the end of the pipet. An oscillation (~40 nm peak-to-peak amplitude at 266.6 Hz herein) normal to the surface in a sinusoidal fashion using a lock-in amplifier (SR830, Stanford Research Instruments) was applied to the pipet while approaching the surface of AM grade HOPG. Upon meniscus contact between the pipet and HOPG substrate, this oscillation introduced a noticeable alternating current (i_{AC}) component of the conductance current due to the periodic deformation of the liquid meniscus. The AC magnitude value was used as a set point to halt the approach of the pipet and as a feedback set point to maintain a constant tip-to-substrate separation during imaging, ensuring that the pipet itself by no means touched the sample physically, but the features on the surface could be readily resolved. During SECCM scans over an area of 10 µm × 10 µm (31 forward and retrace lines, at 0.3 µm s^{-1}, ~30 min scan time), surface topography, electroactivity and conductivity of the solution between the barrels of the probe were recorded simultaneously, leading to maps of various quantities in the probed area. Imaging typically commenced within 15 min of sample cleavage. The data acquisition rate was 389 points per second (each point the average of 256 readings), corresponding to ca.12967 data points per line, and providing > 400000 individual current measurements in the map.

Contact Angle Measurements

Macroscopic measurements of contact angle were carried on HOPG using 5 µL droplets of pure water or a 5 mM $Fe(ClO_4)_3$ in 0.1 M $HClO_4$ aqueous solution, as done in a recent work,[37] but for the studies herein the substrate was unbiased. Measurements were made (solution added to the surface) after different times following HOPG cleavage with the contact angle used as proxy for surface cleanliness and contamination.[35] Images were taken by a camera (PixeLINK PL-B782U, equipped with a 2× magnification lens) with 1920 × 1080 pixels, and analyzed with SPIP (Scanning Probe Image Processor) software package.

AFM Characterization of HOPG Surface

AFM images of freshly cleaved HOPG substrates were captured in air, using an Innova AFM (Bruker), operated in tapping mode with silicon nitride tips.

Results and Discussion

$Fe^{3+/2+}$ Voltammetry on HOPG

It is reported that the $Fe^{3+/2+}$ redox reactions can be affected by certain anions in the solution[30, 32] and this was taken into consideration for the design of experiments, which were carried out in perchlorate medium, as a consequence. On one hand, ClO_4^- was expected to only weakly adsorb on the HOPG electrodes (if at all) and, on the other hand, most of $Fe^{3+/2+}$ ions would remain free in the aqueous solution,[38] in contrast, for example, to SO_4^{2-}, where various ion pairs with $Fe^{3+/2+}$ are formed.[30]

CVs of 5 mM $Fe(ClO_4)_3$ in a supporting electrolyte of 0.1 M $HClO_4$ solution were recorded at a range of scan rates (0.1, 0.5, 1, 2, 3, 4, 5, 6, 7, 8, 9 and 10 V s^{-1}) on freshly cleaved AM and SPI-3 HOPG surfaces. As shown in Figure 2, a pair of redox peaks, due to the reduction of Fe^{3+} and subsequent oxidation of Fe^{2+} that is formed, were observed. Although the step edge coverage is very different (by >2 orders of magnitude) between AM grade and SPI-3 HOPG samples,[5, 15] almost identical (irreversible) voltammetry of $Fe^{3+/2+}$ was seen on these two grades of HOPG. Since the electrochemistry of $Fe^{3+/2+}$ is associated with slow ET kinetics, this indicates unequivocally that step edges have no influence on the ET kinetics, and that ET is dominated by the basal surface.

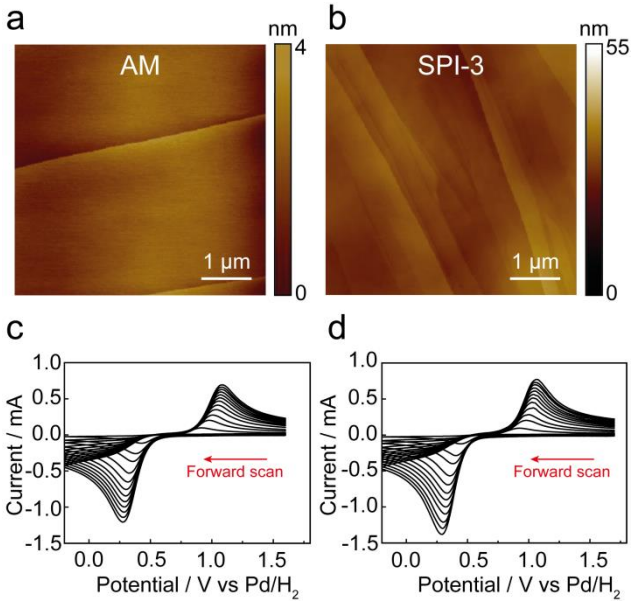

Figure 2. 5 µm × 5 µm tapping-mode AFM images of (a) AM and (b) SPI-3 grade HOPG. Note the difference in scale. Cyclic voltammograms for the reduction of $Fe(ClO_4)_3$ (5 mM in 0.1 M $HClO_4$ solution) on freshly cleaved (c) AM and (d) SPI-3 HOPG. Scan rates: 0.1 (smallest current), 0.5, 1, 2, 3, 4, 5, 6, 7, 8, 9 and 10 (biggest current) V s^{-1}.

Note that the peak-to-peak separation (ΔE_p) of the CVs shown in Figure 2 increased as a function of scan rate, as shown in Figure 3. ΔE_p of 510 ± 19 mV (n = 7) and 498 ± 12 mV (n = 7) were obtained on AM and SPI-3 HOPG, respectively, at a scan rate of 0.1 V s^{-1}, and increased to 801 ± 21 mV (n = 7) and 796 ± 14 mV (n = 7) at 10 V s^{-1}. The similarity of CVs (as determined by ΔE_p values) on these two samples indicated that basal plane HOPG is electroactive toward the ET of $Fe^{3+/2+}$ and that step edges contribute little additional activity.[10, 11, 14]

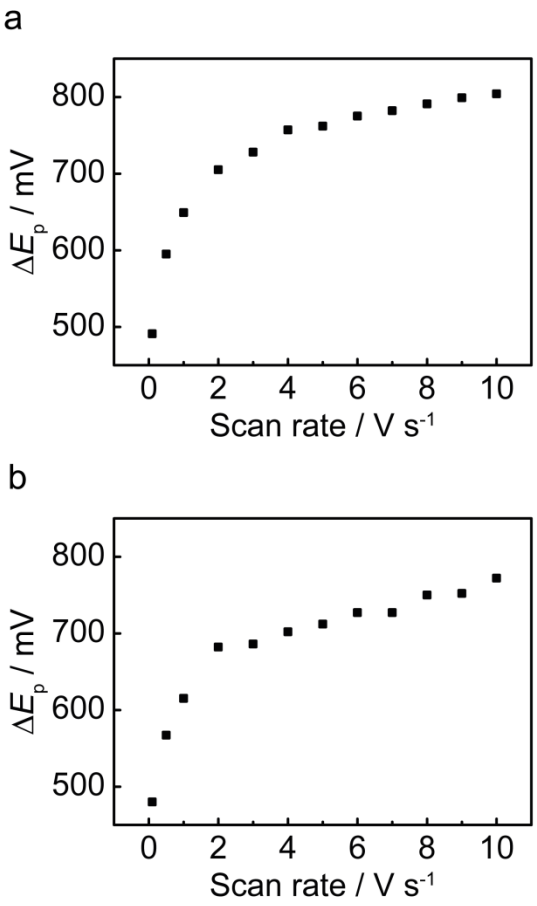

Figure 3. Typical example data of peak-to-peak separation plotted against scan rate for the cyclic voltammograms of 5 mM $Fe(ClO_4)_3$ in 0.1 M $HClO_4$ on (a) AM and (b) SPI-3 HOPG (CV data shown in Figure 2).

The large values of ΔE_p obtained on the CVs were predominantly derived from slow ET kinetics of $Fe^{3+/2+}$ rather than the ohmic drop effects, especially at slow scan rates (although this is considered further below, *vide infra*). A 40-fold decrease in Fe^{3+} concentration (to 0.25 mM in 0.1 M $HClO_4$) produced ΔE_p of 514 ± 3.5 mV (at 0.1 V s^{-1}; n = 3) to 806 ± 4.7 mV (at 10 V s^{-1}; n = 3) on AM grade HOPG (see ESI,† section S1).

FEM simulation of the CVs for the reduction of 5 mM Fe^{3+} (in 0.1 M $HClO_4$) were performed at scan rates of 0.1, 0.5, 1, 5, 7 and 10 V s^{-1} (see ESI,† section S2), using diffusion coefficients $D_O = 4.08\times10^{-6}$ cm^2 s^{-1} for Fe^{3+}, and $D_R = 5.51\times10^{-6}$ cm^2 s^{-1} for Fe^{2+} (adopted from the literature[39]). Ohmic drop effects were not significant for the CVs recorded at a scan rate of 0.1 V s^{-1}, but may be a little more important at fast scan rates (see ESI,† Figure S3). Thus, in the model, 0 and 30 Ω (for AM grade), or 28 Ω (for SPI-3 grade) (reasonable for aqueous solutions in the set up used[18]) of uncompensated resistance were considered for the CVs simulated at 0.1 V s^{-1} and the remainder of the scan rates (0.5, 1, 5, 7 and 10 V s^{-1}), respectively (*vide infra*). As shown in Figure 4, the simulated results matched the experimental data reasonably well on AM and SPI-3 HOPG, in particular at the slow scan rates (i.e. 0.1, 0.5 and 1 V s^{-1}). At fast scan rates (5, 7 and 10 V s^{-1}), the simulation followed the experimental data on AM and SPI-3 HOPG except the post-peak regions where the electrochemical responses were limited by diffusion. Over those areas, the simulated current responses were slightly lower than the experimental CVs, but still in reasonable agreement.

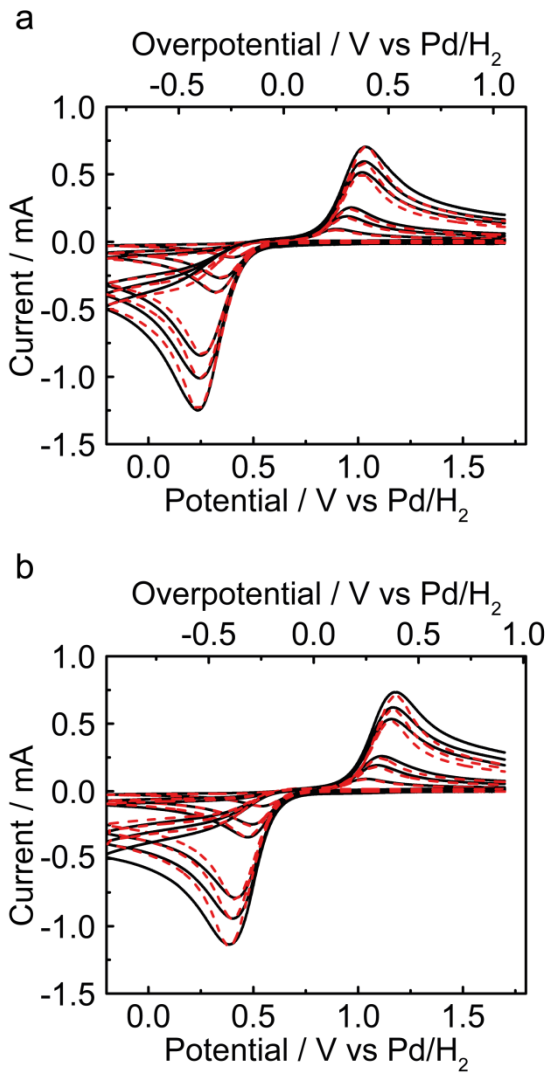

Figure 4. Cyclic voltammograms (black) and simulation results (red) for the reduction of $Fe(ClO_4)_3$ (5 mM in 0.1 M $HClO_4$ solution) on freshly cleaved (a) AM and (b) SPI-3 HOPG. Scan rates: 0.1 (smallest current), 0.5, 1, 5, 7 and 10 (biggest current) V s^{-1}.

Parameters used for the simulations are summarized in Table 1 (see ESI,† section S2). Note that the kinetic term is consistent across the scan rates, but there is a small variation in the area of the droplet, which was allowed to vary by ± 10 % from the measured value. This is because the electrowetting of HOPG can occur at positive potentials during CV scans in some ClO_4^--containing solutions, due to the intercalation/deintercalation of ClO_4^- ions that introduces ClO_4^- ions from the solution into the top graphene layers of HOPG.[37] In the case studied herein, the redox reactions of $Fe^{3+/2+}$ covered a

wide potential window (-0.2 – 1.7 V) that slight electrowetting could just begin to occur at the most positive potentials. Note, however, that intercalation does not occur in the potential region where the kinetics is measured and, even at the maximum extent, the amount of intercalation represents < 1% or less of the surface[37] and so would have a negligible effect on the ET process measured.

Further CV measurements were carried out using an O-ring to confine the droplet cell, in a solution of 0.25 mM Fe^{3+} in 1M $HClO_4$. These results showed slightly larger ΔE_p (see ESI,† section S3). However, it is important to point out that, the O-ring could impose mechanical strain on the surface of HOPG and introduce defects. In general, the mounting of HOPG in any kind of mechanical cell when studying HOPG should be avoid.[5, 40] This again demonstrated the importance of experimental design, to elucidate the ET kinetics on HOPG.

Importantly, there is a good fit in the positions for the redox peaks between simulated and experimental CVs and a kinetic value k_0 of ca. $(5 \pm 1) \times 10^{-5}$ cm s^{-1} was deduced from the simulated curves both for AM and SPI-3 HOPG. This value is within the range of those obtained on metal electrodes (e.g. Pt and Au), i.e. 10^{-5} – 10^{-4} cm s^{-1},[30, 32, 41] which have much higher density of electronic states (DOS) at the intrinsic Fermi level (by > 2 orders of magnitude on Au than HOPG),[11] and also of the same order of magnitude as the upper range obtained on HOPG in previous studies.[36]

Time Effect on the Electrochemical Responses of $Fe^{3+/2+}$ on HOPG

As mentioned in the Introduction, an issue regarding the use of graphite as electrodes can be the contamination on the surfaces by the environment where the substrates are situated.[2, 3, 5, 8, 35, 42-44] It is reported that wettability of carbon materials (graphene and graphite) can be affected by the accumulation of airborne contaminants (mainly hydrocarbons) deposited on the surface with time, as reflected by an increase in contact angle (CA) of aqueous droplets on those surfaces after being exposed to air (with the biggest CA change seen within 10–15 min).[44] Obviously, the time scale of the effect will depend on the environment (cleanliness) and so we also studied the time effect on the wettability of HOPG by placing a droplet of either 5 mM $Fe(ClO_4)_3$ solution (in 0.1 M $HClO_4$) or pure water on AM HOPG surfaces that were cleaved and subsequently exposed in air for different time. As seen from Figure 5, the CA of the $Fe(ClO_4)_3$ solution on freshly cleaved HOPG surface is smaller than observed previously (and also in this study) with pure water (*vide infra*),[9, 37] possibly due to the surface tension changes upon addition of electrolytes,[45] which can influence the CA, according to Young's equation.[46] It was found that the CA of a droplet of a $Fe(ClO_4)_3$ solution increased quite significantly after leaving HOPG for periods up to 30 min, from 42° on freshly cleaved surface of HOPG to 66° on the surface aged for 30 min in air. Beyond that, there was little change in the CA of droplet on HOPG surface with time, indicating that a wettability limit, was achieved.

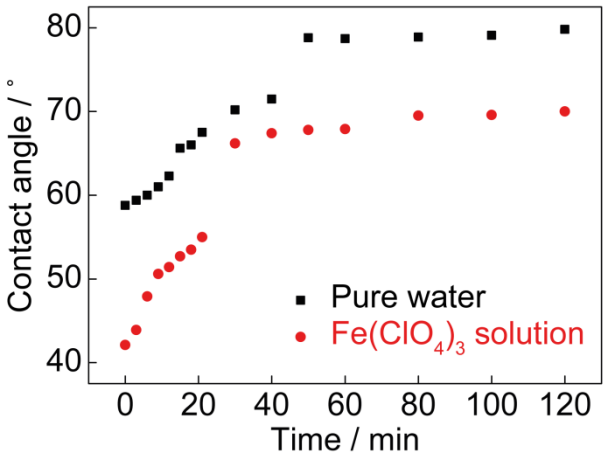

Figure 5. Contact angles of a droplet of pure water (black square) and a 5 mM $Fe(ClO_4)_3$ in 0.1 M $HClO_4$ solution (red dot) on AM HOPG plotted against the time after sample cleavage while being exposed in air.

For comparison, CA measurements were also carried out using droplets of pure water. As seen in Figure 5, on a freshly cleaved surface of AM HOPG the CA was 59°, and it increased significantly with the time of HOPG surface exposure to air. Compared to the droplet of a $Fe(ClO_4)_3$ solution, a longer time (~50 min) was taken for the CA of pure water droplet to reach a stable (and higher) value (~79°).

Considering the fast time scale for the macroscopic CV measurements, carried out within seconds of the cleavage of the HOPG sample in this study (*vide supra*) and our previous studies,[2, 3, 5, 18, 26, 37] surface contamination effects on the ET kinetics will evidently be negligible.

It is interesting to investigate the electrochemical responses of $Fe^{3+/2+}$ redox couple on HOPG as a function of exposure time to the atmosphere, during which the surfaces can possibly change, given that electrochemistry of some other redox couples on graphite electrodes can be potentially affected by time after cleavage of sample.[5, 8] Indeed, some redox species, such as $Fe(CN)_6^{4-/3-}$ and $Ru(NH_3)_6^{3+/2+}$, demonstrated deteriorated responses on aged HOPG samples.[5, 22] In this study, the effect of elapsed time after HOPG cleavage, but before making the electrochemical cell, was tested for $Fe^{3+/2+}$ on AM and SPI-3 HOPG. After cleavage, the surfaces that were left exposed to air for different times, i.e. 0, 10 min, 20 min, 30 min, 1 h, 2h, 4h, and 12 h. Over the period of exposure time, two main possible time-dependent factors (although there may be others) needed to be considered: the accumulation of airborne contaminants on the surface[5, 35] and delamination of top graphene layers from HOPG.[8, 47]

As shown in Figure 6, although the CA of aqueous droplets on HOPG could be significantly affected by surface history (*vide supra*), there was a relatively small difference in the CV responses of $Fe^{3+/2+}$

between freshly cleaved and aged surfaces with the longest exposure time (12 h) in air, for both AM and SPI-3 HOPG samples (*cf*. Figure 2).

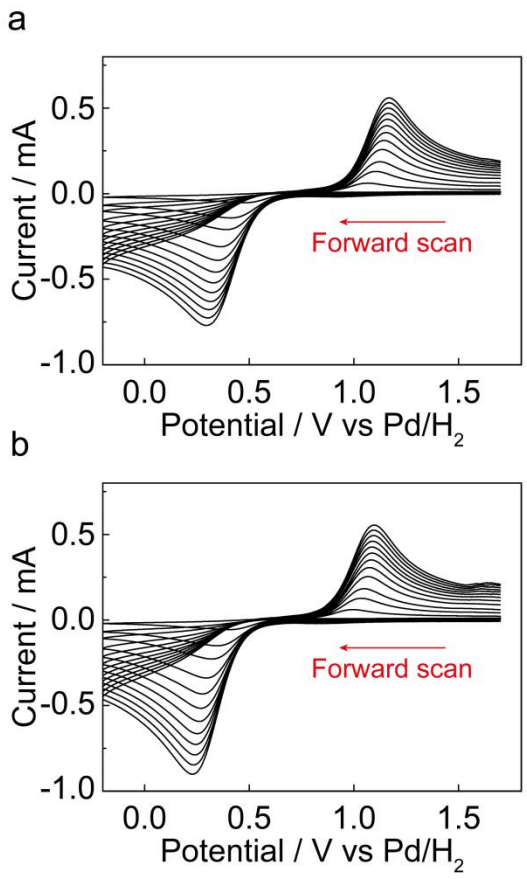

Figure 6. CVs for the reduction of 5 mM $Fe(ClO_4)_3$ (in 0.1 M $HClO_4$ solution) on (a) AM and (b) SPI-3 HOPG that were exposed in air for 12 h after cleavage. Scan rate: 0.1, 0.5, 1, 2, 3, 4, 5, 6, 7, 8, 9 and 10 V s^{-1}.

The ΔE_p values of the CVs for the reduction of Fe^{3+} on fresh and aged AM and SPI-3 HOPG surfaces are plotted against exposure time in Figure 7. Given the possible ohmic drop effect at fast scan rates (*vide supra*), only the CVs at the three slowest scan rates (0.1, 0.5 and 1 V s^{-1}) were considered. As seen in Figure 7, the ΔE_p increased gradually with the exposure time of the HOPG surface to the atmosphere for all three scan rates, and changed by ~100 mV on HOPG surface that was exposed in air for 12 h after cleavage.

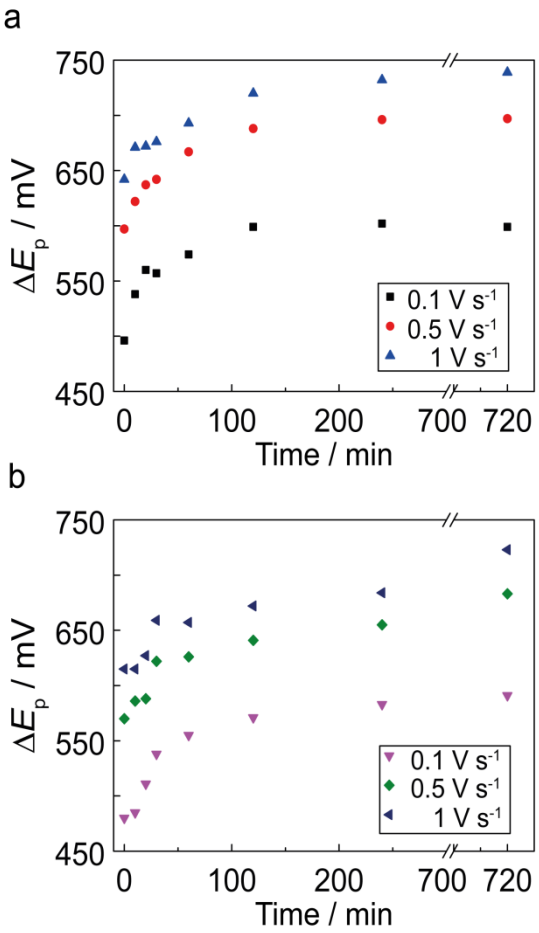

Figure 7. Peak-to-peak separation, ΔE_p, of CVs for the reduction of 5 mM $Fe(ClO_4)_3$ (in 0.1 M $HClO_4$ solution) plotted against the time after cleavage for (a) AM and (b) SPI-3 HOPG. CVs data at 0.1, 0.5 and 1 V s^{-1}.

The k_0 values can be readily estimated from ΔE_p of CVs (shown in Figure 7) by using the equation developed by Klingler and Kochi (assume the transfer coefficient = 0.5).[48] As shown in Figure 8, k_0 of 4.9×10^{-5} cm s^{-1} and 5.8×10^{-5} cm s^{-1} were obtained for the CVs recorded at 0.1 V s^{-1} on freshly cleaved AM and SPI-3 grade HOPG, respectively, with 4.1×10^{-5} cm s^{-1} and 5.4×10^{-5} cm s^{-1} correspondingly observed at 0.5 V s^{-1}, and 3.8×10^{-5} cm s^{-1} and 4.9×10^{-5} cm s^{-1} at 1 V s^{-1}. These values are in good accordance with simulation results (*vide supra*), and different scan rates led to similar k_0 values. The slightly higher k_0 values on SPI-3 grade HOPG, as also seen in the CV simulations, correlates with the higher specific surface area for this electrode (higher step edge density), but not higher intrinsic kinetics at the edges. The k_0 values decreased with the elapsed time after cleavage of HOPG and tended to be constant after ~1 h on the two grades of HOPG. With an exposure time of 12 h (the longest time considered in this study), the aged HOPG surfaces displayed kinetic values (from 0.1 V s^{-1}) of $k_0 = 1.8 \times 10^{-5}$ cm s^{-1} for AM grade and $k_0 = 2 \times 10^{-5}$ cm s^{-1} for SPI-3 grade. Given the long extent of surface exposure, which would lead to significant changes in the surface, due to possible contamination,

delamination, surface oxidation, doping and other processes, the effect on the kinetics is actually relatively small. Interestingly, these k_0 values are similar to those that have been proposed as characteristic of high quality HOPG,[11, 36] and as we have pointed out before,[2, 3, 5] those measurements[11, 36] may be compromised by contamination or other effects, such as delamination of the top surface layers,[5,8] depending on the method of cleavage.

Regarding the possible effects from delamination of the top layers of graphene from graphite that may occur with time,[5, 8] the redox potential for $Fe^{3+/2+}$ is far from the intrinsic Fermi level of graphite (and graphene; -0.2 V vs Ag/AgCl),[11] and as a result, the $Fe^{3+/2+}$ redox process may not be as strongly affected by time-dependent (decoupling) structural changes. As the k_0 values measured herein on freshly cleaved HOPG are similar to metal electrodes, even though the DOS at HOPG is much lower than on metal electrodes,[11] the electrochemistry of the outer-sphere $Fe^{3+/2+}$ shows an adiabatic behaviour.

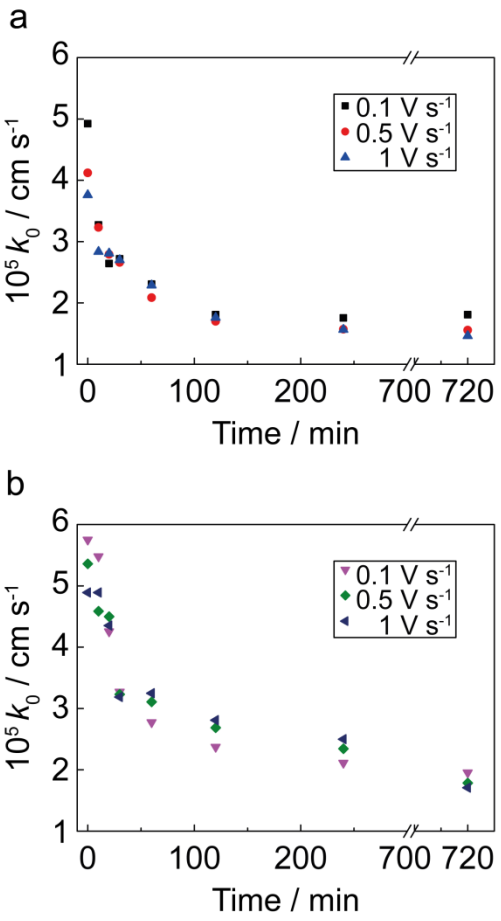

Figure 8. Standard heterogeneous rate constant (k_0), obtained from ΔE_p values of CVs shown in Figure 7, plotted as a function of the time after exposure to air for (a) AM and (b) SPI-3 HOPG electrodes. Three scan rates (0.1, 0.5 and 1 V s^{-1}) were considered for the CVs obtained with 5 mM $Fe(ClO_4)_3$ in 0.1 M $HClO_4$ solution.

SECCM Electrochemical Imaging of AM HOPG Surface

As we have shown in many studies,[2, 5, 7, 8, 20, 33] SECCM is a powerful technique that enables surface electroactivity to be mapped with high temporal and spatial resolution. An advantage of this technique is that measurements can be done shortly after sample preparation (typically within 15 min), minimizing surface history effects for many systems. In the case of HOPG, the electroactivity of basal plane alone, or basal plane with intersecting step edges, can be probed separately by a small SECCM pipet, with the working electrode area confined by the meniscus contact.[25] SECCM experiments were carried out on a cleaved AM HOPG surface, using a solution of 0.1 M $HClO_4$ containing 2 mM $Fe(ClO_4)_2$, to investigate the electroactivity of different (localised) surface features. A typical SECCM CV for the one–electron oxidation of Fe^{2+} (at 0.1 V s^{-1}) on the basal plane is shown in Figure 9a, where a sigmoidal response for nonlinear (spherical segment) diffusion is observed,[49] due to the significantly enhanced mass transport in the tapered pipet, and under a bias applied between the barrels.[50, 51] The value of potential difference between the 3/4 and 1/4-wave potentials ($E_{3/4}$-$E_{1/4}$) was ~120 mV, and half-wave potential $E_{1/2}$ was shifted anodically by 397 mV from the formal potential, indicative of the irreversibility of CVs and slow ET kinetics of $Fe^{3+/2+}$ on HOPG.[49] The standard ET rate constant, k_0, was found to be ~7.4×10^{-5} cm s^{-1}, very close to that obtained from simulation of macroscopic CV measurements on the freshly cleaved surface, indicating that the SECCM measurements relate closely to a pristine surface (see ESI,† section S4).

SECCM mapping was performed at about 1.2 V (vs Pd/H_2), at the foot of the wave where any differences in ET kinetics across the surface would be most revealed. In Figure 9b, it should be noted that the first several lines of the image demonstrated slightly higher surface current than the rest of the area probed, which might be due to the electrowetting occurring at positive potentials, as seen for the droplets of perchlorate and sulfate salt solutions on HOPG.[37] This was evidenced by the slightly larger values of the corresponding ion conductance current in this region (see ESI,† section S5). After the stabilisation of the meniscus, little variation in surface current was observed across the probed area. Only slightly higher currents were seen at some areas of step edges. Measurements on an aged AM HOPG surface (>2 h in air after cleavage) showed similar behaviour. In part, this could be due to enhanced meniscus wetting at step edges, as a result of negative charge (functionality) at steps.[52] Slightly higher activity at edges cannot be ruled out completely, but any effect would be very small, based on the macroscopic measurements reported above. Importantly, SECCM mapping of HOPG surface shows that the basal plane HOPG is the predominant site for the ET of $Fe^{3+/2+}$ and is the main feature responsible for the overall behaviour seen in HOPG voltammetry.

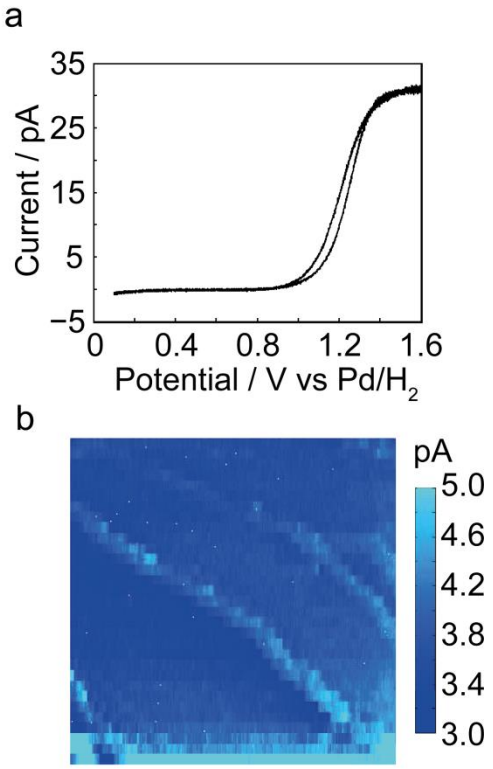

Figure 9. (a) A typical CV for the oxidation of 2 mM Fe^{2+} in 0.1 M $HClO_4$, recorded at 0.1 V s^{-1} and (b) SECCM electrochemical activity map of an area of 10 µm × 10 µm on a cleaved AM HOPG surface.

Conclusions

The electrochemical behaviour of $Fe^{3+/2+}$ redox couple on HOPG has been studied at the macroscale and nanoscale. The standard heterogeneous ET rate constant of $Fe^{3+/2+}$ on HOPG, k_0 ~5×10^{-5} cm s^{-1}, deduced from simulations of macroscopic CV results, fell in the range of values obtained for metal electrodes (e.g. Pt and Au) and step edge coverage had little effect on the voltammetric responses and ET kinetics. This was further supported by SECCM electroactivity mapping of HOPG surface, where uniform activity of the basal surface of HOPG for the ET of $Fe^{3+/2+}$ was revealed (k_0 ~ 7.4×10^{-5} cm s^{-1}). The basal plane is the major electroactive site on cleaved HOPG.

Considering the similar k_0 values obtained for $Fe^{3+/2+}$ on graphite and metal electrodes, and the noticeable difference in DOS between these materials,[11] the DOS does not appear to have much impact on the ET kinetics of $Fe^{3+/2+}$ for the range of DOS values encompassed by HOPG and metals. This is in line with our results for some other outer-sphere redox species on HOPG,[2, 3, 18] and adds to an expanding body of work that the DOS does not play a generally important role in outer-sphere redox process, i.e. that these processes may be considered to be adiabatic. The $Fe^{3+/2+}$ couple has been studied less in comparison to other outer-sphere redox probes, such as $Fe(CN)_6^{3-/4-}$, which is actually more problematic for a number of reasons.[5] We would recommend that it could be considered and used more often for the comparison of different electrode materials. An advantage of the $Fe^{3+/3+}$ couple is that the slow kinetics means that quite simple and straightforward electrochemical methods can be used for quantitative studies.

The surface history of HOPG (exposure in air after cleavage) was explored. Exposure to air affects the wettability of HOPG, as evidenced by the increase of the aqueous contact angle on increasingly aged HOPG. There is an associated decrease in the ET kinetics of $Fe^{3+/2+}$, although even on surfaces exposed to air for 12 h, the k_0 values are still of the same order (a factor of 2 or 3 lower) than on freshly-cleaved HOPG surface.

Acknowledgements

This work was funded by the European Research Council (ERC-2009-AdG 247143-QUANTIF). G.Z acknowledges support by a Chancellor's International Scholarship at the University of Warwick. We are grateful to Prof. R. L. McCreery for kindly providing HOPG samples for the research. Some equipment used in this research was obtained through Birmingham Science City with support from Advantage West Midlands and the European Regional Development Fund.

Notes and references

1. H. V. Patten, M. Velický and R. A. W. Dryfe, in *Electrochemistry of Carbon Electrodes*, Wiley-VCH Verlag GmbH & Co. KGaA, 2015, ch4, pp. 121-162.
2. P. R. Unwin, A. G. Guell and G. Zhang, *Acc Chem Res*, 2016, **49**, 2041-2048.
3. A. G. Güell, S.-y. Tan, P. R. Unwin and G. Zhang, in *Electrochemistry of Carbon Electrodes*, Wiley-VCH Verlag GmbH & Co. KGaA, 2015, ch2, pp. 31-82.
4. J. V. Macpherson, *Phys. Chem. Chem. Phys.*, 2015, **17**, 2935-2949.
5. A. N. Patel, M. G. Collignon, M. A. O'Connell, W. O. Hung, K. McKelvey, J. V. Macpherson and P. R. Unwin, *J. Am. Chem. Soc.*, 2012, **134**, 20117-20130.
6. F. Gloaguen, J. M. Léger, C. Lamy, A. Marmann, U. Stimming and R. Vogel, *Electrochim. Acta*, 1999, **44**, 1805-1816.
7. A. G. Güell, K. E. Meadows, P. V. Dudin, N. Ebejer, J. V. Macpherson and P. R. Unwin, *Nano Lett.*, 2014, **14**, 220-224.
8. A. G. Güell, A. S. Cuharuc, Y. R. Kim, G. Zhang, S. Y. Tan, N. Ebejer and P. R. Unwin, *ACS Nano*, 2015, **9**, 3558-3571.
9. A. Ashraf, Y. Wu, M. C. Wang, N. R. Aluru, S. A. Dastgheib and S. Nam, *Langmuir*, 2014, **30**, 12827-12836.
10. R. L. McCreery and M. T. McDermott, *Anal. Chem.*, 2012, **84**, 2602-2605.
11. K. K. Cline, M. T. McDermott and R. L. McCreery, *J. Phys. Chem.*, 1994, **98**, 5314-5319.
12. R. J. Rice and R. L. McCreery, *Anal. Chem.*, 1989, **61**, 1637-1641.
13. T. J. Davies, M. E. Hyde and R. G. Compton, *Angew. Chem. Int. Ed.*, 2005, **44**, 5121-5126.
14. C. E. Banks, T. J. Davies, G. G. Wildgoose and R. G. Compton, *Chem. Commun.*, 2005, 829-841.
15. A. N. Patel, S. Y. Tan and P. R. Unwin, *Chem. Commun.*, 2013, **49**, 8776-8778.
16. A. N. Patel, K. McKelvey and P. R. Unwin, *J. Am. Chem. Soc.*, 2012, **134**, 20246-20249.
17. G. Zhang, P. M. Kirkman, A. N. Patel, A. S. Cuharuc, K. McKelvey and P. R. Unwin, *J. Am. Chem. Soc.*, 2014, **136**, 11444-11451.
18. G. Zhang, A. S. Cuharuc, A. G. Güell and P. R. Unwin, *Phys. Chem. Chem. Phys.*, 2015, **17**, 11827-11838.
19. A. N. Patel, S. Y. Tan, T. S. Miller, J. V. Macpherson and P. R. Unwin, *Anal. Chem.*, 2013, **85**, 11755-11764.
20. S. C. S. Lai, A. N. Patel, K. McKelvey and P. R. Unwin, *Angew. Chem. Int. Ed.*, 2012, **51**, 5405-5408.
21. A. Anne, E. Cambril, A. Chovin, C. Demaille and C. Goyer, *ACS Nano*, 2009, **3**, 2927-2940.
22. P. L. Frederix, P. D. Bosshart, T. Akiyama, M. Chami, M. R. Gullo, J. J. Blackstock, K. Dooleweerdt, N. F. de Rooij, U. Staufer and A. Engel, *Nanotechnology*, 2008, **19**, 384004.
23. A. J. Wain, A. J. Pollard and C. Richter, *Anal. Chem.*, 2014, **86**, 5143-5149.
24. S. C. S. Lai, R. A. Lazenby, P. M. Kirkman and P. R. Unwin, *Chem. Sci.*, 2015, **6**, 1126-1138.
25. C. G. Williams, M. A. Edwards, A. L. Colley, J. V. Macpherson and P. R. Unwin, *Anal. Chem.*, 2009, **81**, 2486-2495.
26. A. S. Cuharuc, G. Zhang and P. R. Unwin, *Phys. Chem. Chem. Phys.*, 2016, **18**, 4966-4977.
27. Y. Niimi, T. Matsui, H. Kambara, K. Tagami, M. Tsukada and H. Fukuyama, *Phys. Rev. B*, 2006, **73**, 085421.
28. Y. Kobayashi, K.-i. Fukui, T. Enoki, K. Kusakabe and Y. Kaburagi, *Phys. Rev. B*, 2005, **71**, 193406.
29. W. Schmickler and E. Santos, *Interfacial Electrochemistry*, Springer-Verlag Berlin Heidelberg, 2 edn., 2010.
30. B. D. B. Aaronson, C.-H. Chen, H. Li, M. T. M. Koper, S. C. S. Lai and P. R. Unwin, *J. Am. Chem. Soc.*, 2013, **135**, 3873-3880.
31. D. C. Johnson and E. W. Resnick, *Anal. Chem.*, 1977, **49**, 1918-1924.
32. J. Weber, Z. Samec and V. Mareček, *J. Electroanal. Chem.*, 1978, **89**, 271-288.
33. N. Ebejer, A. G. Güell, S. C. Lai, K. McKelvey, M. E. Snowden and P. R. Unwin, *Annu. Rev. Anal. Chem.* , 2013, **6**, 329-351.
34. N. Ebejer, M. Schnippering, A. W. Colburn, M. A. Edwards and P. R. Unwin, *Anal. Chem.*, 2010, **82**, 9141-9145.
35. Z. Li, Y. Wang, A. Kozbial, G. Shenoy, F. Zhou, R. McGinley, P. Ireland, B. Morganstein, A. Kunkel, S. P. Surwade, L. Li and H. Liu, *Nat. Mater.*, 2013, **12**, 925-931.
36. C. A. McDermott, K. R. Kneten and R. L. McCreery, *J. Electrochem. Soc.*, 1993, **140**, 2593-2599.
37. G. Zhang, M. Walker and P. R. Unwin, *Langmuir*, 2016, **32**, 7476-7484.
38. J. Sutton, *Nature*, 1952, **169**, 71-72.
39. R. J. Taylor and A. A. Humffray, *J. Electroanal. Chem.*, 1973, **42**, 347-354.
40. M. T. McDermott, K. Kneten and R. L. McCreery, *J. Phys. Chem.*, 1992, **96**, 3124-3130.
41. D. H. Angell and T. Dickinson, *J. Electroanal. Chem.*, 1972, **35**, 55-72.
42. N. Nioradze, R. Chen, N. Kurapati, A. Khvataeva-Domanov, S. Mabic and S. Amemiya, *Anal. Chem.*, 2015, **87**, 4836-4843.
43. Z. Li, A. Kozbial, N. Nioradze, D. Parobek, G. J. Shenoy, M. Salim, S. Amemiya, L. Li and H. Liu, *ACS Nano*, 2016, **10**, 349-359.
44. A. Kozbial, Z. Li, J. Sun, X. Gong, F. Zhou, Y. Wang, H. Xu, H. Liu and L. Li, *Carbon*, 2014, **74**, 218-225.
45. P. K. Weissenborn and R. J. Pugh, *J. Colloid Interface Sci.*, 1996, **184**, 550-563.
46. D. Klarman, D. Andelman and M. Urbakh, *Langmuir*, 2011, **27**, 6031-6041.
47. G. Li, A. Luican and E. Y. Andrei, *Phys. Rev. Lett.*, 2009, **102**, 176804.
48. R. J. Klingler and J. K. Kochi, *J. Phys. Chem.*, 1981, **85**, 1731-1741.
49. A. J. Bard and L. R. Faulkner, *Electrochemical Methods: Fundamentals and Applications*, John Wiley& Sons, Inc., New York, 2nd edn., 2001.
50. M. E. Snowden, A. G. Güell, S. C. Lai, K. McKelvey, N. Ebejer, M. A. O'Connell, A. W. Colburn and P. R. Unwin, *Anal. Chem.*, 2012, **84**, 2483-2491.
51. D. Momotenko, J. C. Byers, K. McKelvey, M. Kang and P. R. Unwin, *ACS Nano*, 2015, **9**, 8942-8952.
52. R. Koestner, Y. Roiter, I. Kozhinova and S. Minko, *J. Phys. Chem. C*, 2011, **115**, 16019-16026.

Graphical abstract

Electron transfer kinetics of $Fe^{3+/2+}$ on HOPG is similar to metal electrodes but influenced by long exposure to ambient.